Design of whey protein aggregates towards microgel-stabilized emulsion generation

Ignacio Niizawa [*], Guillermo A. Sihufe, Susana E. Zorrilla

Instituto de Desarrollo Tecnológico para la Industria Química (INTEC), Universidad Nacional del Litoral (UNL) - Consejo Nacional de Investigaciones Científicas y Técnicas (CONICET), Güemes 3450 (S3000GLN), Santa Fe, Argentina

ARTICLE INFO

ABSTRACT

Whey protein aggregates (WPAg) were designed from whey protein concentrate suspensions adjusting thermal treatment conditions to prepare microgel-stabilized emulsions. The response surface methodology (RSM) was used to design WPAg with different characteristics (size, denaturation degree, and exposure degree of surface thiol groups), considering the effect of temperature (67.9 °C - 83.1 °C), protein concentration (3.49% w/w - 6.01% w/w), and pH (6.49 - 7.76) conditions throughout the thermal aggregation process. Three types of WPAg with markedly different characteristics were obtained using the RSM models to evaluate the influence of different protein aggregates on microgel-stabilized emulsions. These microgel particles successfully stabilized the emulsions against coalescence during 14 days of storage, particularly at pH 4.7 and 7.

1. Introduction

Whey proteins (WP) are the soluble protein fraction in milk, including principally β-lactoglobulin, α-lactalbumin, and bovine serum albumin, which comprise almost 50%, 20%, and 6% of the total protein content, respectively (Wijayanti, Bansal, & Deeth, 2014).

Whey protein aggregates (WPAg) can be produced by heating WP above their denaturation temperature (>60 °C). Different structural and functional properties of WPAg can be obtained by adjusting the processing conditions such as pH, heating time, temperature, protein concentration, and presence of ions (Ryan, Zhong, & Foegeding, 2013). Whey protein aggregates can be considered microgels because consist of a crosslinked network of WP containing a large amount of solvent (Dickinson, 2015; Ryan & Foegeding, 2015; Schmitt, Bovay, Vuilliomenet, Rouvet, & Bovetto, 2011).

The use of WPAg to stabilize emulsions (WP microgel-stabilized emulsions) has gained interest due to their combined advantages of biocompatibility and a high degree of resistance to coalescence (Destribats, Rouvet, Gehin-Delval, Schmitt, & Binks, 2014). The WP microgel particles may form a single dense layer at the contact area between two droplets, preventing droplets from coalescing (Dybowska & Krupa-Kozak, 2020; Nicolai, 2016). Moreover, these "smart" colloids can respond rapidly to environmental changes (temperature, pH, addition of solutes, etc.) because of the high surface-to-volume ratio of microgels and their special sensitivity to swelling or shrinkage under the influence of external stimuli (Dickinson, 2015). Well-defined purified ingredients like β-lactoglobulin or whey protein isolates (WPI) are generally used to obtain the WPAg (Destribats et al., 2014; Murphy, Zhu, Narsimhan, & Jones, 2018; Nicolai, 2016; Ramos et al., 2017; Sarkar et al., 2016). The use of whey protein concentrate (WPC) is less common due to its lower degree of purity. However, its economic advantage over WPI makes WPC an interesting alternative.

The purpose of the present work was to develop food-grade microgel particles from WPC to stabilize soy oil emulsions. The objectives were to determine the influence of temperature, protein concentration and pH on the characteristics of WPAg (size, denaturation degree, and exposure degree of surface thiol groups), and to investigate the ability of the obtained WPAg in the formation and stabilization of soy o/w emulsions.

2. Materials and methods

2.1. Preparation of whey protein aggregates by thermal treatment

Whey protein suspensions used for WPAg preparation were obtained from a commercial WPC powder (LACPRODAN 80, Arla Foods Ingredients SA, Córdoba, Argentina) previously used by the research group (Meza et al., 2020). The protein content (74.4 ± 0.9% w/w) was estimated in duplicate using the Kjeldahl method with a nitrogen

---

conversion factor of 6.38 (Büchi Labortechnik AG, 1998). The moisture content (4.8 ± 0.6% w/w) was determined in duplicate with a microwave CEM AVC 80 (CEM, Matthews, NC, USA). Lactose (7 ± 2% w/w), fat (max. 8% w/w), and ash (max. 3.5% w/w) content were provided by the manufacturer. The calcium content (0.359 ± 0.001 mg g^{-1}) was determined by atomic absorption spectroscopy.

The necessary amount of WPC was dissolved in 120 mL of ultrapure water to obtain the desired protein concentration (according to section 2.2). Whey protein concentrate suspensions were stirred for 1 h at room temperature (25 °C) and stored overnight at 4 °C to ensure the complete hydration of proteins. The next day, pH was adjusted (according to section 2.2) at room temperature (25 °C) using 1 mol L^{-1} NaOH or 1 mol L^{-1} HCl. Then, WPC suspensions were poured into glass tubes (1 cm in external diameter, 0.9 cm in internal diameter and 10 cm in height) and sealed with plastic caps to avoid evaporation. Whey protein concentrate suspensions were heated at the selected temperature (according to section 2.2) using a HAAKE N3 water bath (HAAKE, Berlin, Germany) for different time intervals (0, 3, 6, 9, 12, 15, 30, 45 and 60 min) in triplicate. Glass tubes were immersed in an ice bath for 5 min to stop the heat treatment. The samples were stored at 4 °C overnight for further analysis.

2.2. Experimental design for thermal aggregation process modeling

Whey protein aggregates with different structural and functional properties can be obtained by adjusting the process conditions during thermal aggregation. In this work, three independent variables were used (temperature, pH and protein concentration) to promote protein aggregation (microgel particles) but avoiding further association of WP, which produces macroscopic gels. The ranges for each variable were selected based on literature (Nicolai, 2016; Nicolai, Britten, & Schmitt, 2011; Nicolai & Durand, 2013; Zhang, Arrighi, Campbell, Lonchamp, & Euston, 2016) and on previous results of our research group (Meza et al., 2020).

Response surface methodology is a collection of mathematical and statistical methods used to model and optimize the processes in which response variables are affected by multiple independent variables, alone or in combination (Zou & Akoh, 2013). The response surface methodology was used for estimating the effect of the three independent variables on the WPAg characteristics. A central-composite design was proposed, consisting of 19 experiments including 8 factorial, 6 axial, and 5 central points (Table 1).

The experimental data obtained was fitted with a polynomial model for predicting the response of the dependent variables according to Eq. (1):

Table 1
Central-composite design for WP thermal aggregation process analysis.

Run	Temperature (°C)	Protein Concentration (% w/w)	pH
1	71.0	4.00	6.75
2	80.0	4.00	6.75
3	71.0	5.50	6.75
4	80.0	5.50	6.75
5	71.0	4.00	7.50
6	80.0	4.00	7.50
7	71.0	5.50	7.50
8	80.0	5.50	7.50
9	67.9	4.75	7.13
10	83.1	4.75	7.13
11	75.5	3.49	7.13
12	75.5	6.01	7.13
13	75.5	4.75	6.49
14	75.5	4.75	7.76
15	75.5	4.75	7.13
16	75.5	4.75	7.13
17	75.5	4.75	7.13
18	75.5	4.75	7.13
19	75.5	4.75	7.13

$$Y_m = \beta_0 + \sum_{i=1}^{k} \beta_i X_i + \sum_{i=1}^{k} \beta_{ii} X_i^2 + \sum_{i=1}^{k} \sum_{j=i+1}^{k} \beta_{ij} X_i X_j \qquad (1)$$

where Y_m is the dependent variable analyzed; β_0 is a constant coefficient; β_i, β_{ii} and β_{ij} are the coefficients for linear, quadratic and interaction effect, respectively; and X_i and X_j are the independent variables. The linear terms analyze the effect of one factor at a time over the response studied, while the interaction terms evaluate the effect of two factors simultaneously. The quadratic terms investigate a non-linear response. The sign and magnitude of each significant factor in the quadratic equation denote its relative influence on the dependent response evaluated. Multiple response optimization was analyzed by Design-Expert 7.0 statistical software (Stat Ease, Inc., Minnesota, USA).

2.3. Whey protein aggregates characterization

The effects of the thermal aggregation process conditions (temperature, pH and protein concentration) on the WPAg size, WP denaturation rate and WP thiol surface group exposure were analyzed.

2.3.1. Size of whey protein aggregates

The average particle diameter of WPAg produced by thermal aggregation treatments was measured in triplicate by dynamic light scattering (DLS) with 90° detection optics using a BI-9000 AT equipment (Brookhaven Instruments, Holtsville, New York, USA) (Mourouzidis-Mourouzis & Karabelas, 2006). The measurements were carried out at 30 °C. The WPAg concentration was adjusted using ultrapure water to produce a counting rate between 40,000–120,000 counts s^{-1}.

2.3.2. Whey protein denaturation during the thermal aggregation process

Protein solubility affects its functional food applications in the industry. It depends on the balance between repulsive and attractive intermolecular forces. The protein denaturation process was studied analyzing the soluble protein (SP) content of WP suspensions as suggested by Meza, Verdini, and Rubiolo (2009). Throughout the thermal aggregation process, different aliquots of each WP suspension were taken in triplicate and the pH was adjusted to 4.6 ± 0.1 using 1 mol L^{-1} HCl or 1 mol L^{-1} NaOH to induce the precipitation of denatured/aggregated WP near their isoelectric point (IEP) (de Wit, 1990; Li-Chan, 1983). Then, samples were centrifuged for 30 min at 5 °C and 26,000 g in a Biofuge 28RS centrifuge (Heraeus Sepatech, Osterode, Germany). The SP content in the supernatants was determined by measuring absorption at 280 nm after appropriate dilution in a dissociating buffer (50 mmol L^{-1} EDTA, 8 mol L^{-1} urea, pH 10) using a Genesys 5 spectrophotometer (Milton Roy Company, Rochester, NY). The insoluble protein content of suspensions at pH 4.6 was defined as the difference between total protein (TP) and SP contents and was used to estimate the extent of denaturation/aggregation of whey proteins. The percentage of denatured proteins (DP) content was calculated according to the following equation:

$$DP[\%] = [(TP - SP) / TP] \times 100 \qquad (2)$$

Changes in protein denaturation as a function of heating time were described by a first-order kinetic model:

$$DP_t[\%] = DP_{t\infty} + \left(DP_{t_0} - DP_{t_\infty}\right) \exp^{-k_{DP} t} \qquad (3)$$

where $DP_{t\infty}$ is the equilibrium value of DP at infinite heating time, DP_{t0} is the value of DP at initial heating time and k_{DP} is the constant associated with protein denaturation rate. Kinetic parameters were estimated from experimental results by non-linear regression analysis. Constant k_{DP} was used to calculate the average time to achieve the denaturation of 50% of total WP available ($t_{1/2}$) as a parameter to study the influence of the three independent variables over protein denaturation kinetic under the thermal process.

Table 2
Statistics summary of the quadratic response surface models for Y_1, Y_2, and Y_3.

Response	Model						Lack of fit	
	F - Value	Prob > F	R^2	Adj. R^2	Adeq. prec.	C.V. (%)	F - Value	Prob > F
Y_1	62.58	<0.0001	0.97	0.95	26.83	8.60	0.31	0.9232
Y_2	186.26	<0.0001	0.99	0.98	48.58	6.64	2.09	0.2494
Y_3	103.48	<0.0001	0.99	0.95	34.26	8.85	0.57	0.7876

Table 3
The experimental (mean $\pm$ SD, n = 3) and predicted values for responses Y_1, Y_2 and Y_3 for the test conditions.

Run	Y_1 - WPAg size (nm)		Y_2 - $t_{1/2}$ (min)		Y_3 - k_{SH} x10^{-2} (min^{-1})	
	Experimental	Predicted	Experimental	Predicted	Experimental	Predicted
1	437.2 ± 11.0	434.4	1.7 ± 0.2	1.8	3.18 ± 0.82	2.88
2	784.4 ± 9.0	731.5	9.5 ± 0.2	9.3	14.30 ± 2.18	15.85
3	531.4 ± 24.6	512.4	12.9 ± 1.5	13.2	1.64 ± 0.73	2.09
4	1421.3 ± 45.8	1144.8	2.8 ± 0.2	3.0	11.29 ± 1.90	11.48
5	324.2 ± 8.9	319.1	4.4 ± 0.7	4.8	4.73 ± 0.06	4.47
6	364.9 ± 7.9	345.4	4.8 ± 0.3	4.8	28.45 ± 9.45	24.55
7	356.2 ± 9.9	352.0	4.3 ± 0.2	4.8	5.58 ± 1.08	5.62
8	388.3 ± 17.6	386.4	3.7 ± 0.1	4.2	29.89 ± 3.62	30.90
9	341.2 ± 12.1	343.7	1.8 ± 0.1	1.6	0.93 ± 0.41	0.89
10	465.6 ± 18.3	497.0	7.1 ± 0.4	7.1	45.11 ± 14.46	*
11	357.3 ± 20.9	364.1	5.6 ± 0.1	5.5	10.84 ± 1.59	13.18
12	454.9 ± 5.2	454.1	4.5 ± 0.1	4.8	13.88 ± 0.06	12.30
13	1293.9 ± 67.5	1614.6	19.5 ± 0.7	17.0	8.65 ± 1.62	6.92
14	329.7 ± 5.1	339.7	30.2 ± 0.6	34.7	22.57 ± 2.17	22.91
15	373.7 ± 14.5	402.9	3.4 ± 0.1	3.3	12.90 ± 0.93	12.59
16	370.8 ± 10.8	402.9	3.0 ± 0.3	3.0	12.36 ± 0.66	12.59
17	406.5 ± 5.5	402.9	21.4 ± 0.9	17.8	12.70 ± 0.42	12.59
18	431.9 ± 10.5	402.9	2.5 ± 0.2	2.3	17.62 ± 0.74	12.59
19	421.1 ± 19.5	402.9	5.2 ± 0.2	4.8	8.56 ± 0.71	12.59

* Outlier of the model.

2.3.3. Kinetic study of thiol surface group exposure during the thermal aggregation process

The exposed and total SH groups of WP suspensions were determined during the thermal treatments as suggested by Sava, Van der Plancken, Claeys, and Hendrickx (2005). The tests were performed in triplicate.

Aliquots of protein suspensions taken throughout the thermal process were diluted with appropriate buffer solution and Ellman's reagent (5,5'-dithiobis-(2-nitrobenzoic acid) (4 mg mL^{-1}) was added. For surface SH groups, the buffer composition was: 86 mmol L^{-1} Tris, 90 mmol L^{-1} glycine and 4 mmol L^{-1} EDTA at pH 8.0. While for total SH groups the buffer composition was: 86 mmol L^{-1} Tris, 90 mmol L^{-1} glycine, 4 mmol L^{-1} EDTA and 8 mol L^{-1} urea at pH 8.0. The absorbance at 412 nm was measured against a reagent blank after 2 min (total SH groups) or 15 min (surface SH groups) at 20 °C. The total SH groups were calculated with Eq. (4):

$$SH_{Tot}[\mu mol\ SH\ /\ gr\ protein] = (Abs_1 - Abs_0)\ /\ (c\ 13600) \qquad (4)$$

where Abs_1 is the absorbance of heat-treated sample at 412 nm, Abs_0 is the absorbance of the control, 13,600 is the molar extinction coefficient (mol^{-1} L cm^{-1}) and c is the protein concentration (mg mL^{-1}).

The surface SH groups were calculated with Eq. (5):

$$SH_{Surf}[\%] = [(Abs_1 - Abs_0)/(c\ 13600)]\ (100/SH_{Tot}) \qquad (5)$$

Changes in surface thiol availability as a function of heating time can be described by a first-order kinetic model (Sava et al., 2005):

$$SH_{Surf,t}[\%] = SH_{t\infty} + (SH_{t0} - SH_{t\infty})\ \exp^{-k_{SH}\ t} \qquad (6)$$

where $SH_{t\infty}$ is the equilibrium value of surface SH at infinite heating time, SH_{t0} is the value of surface SH at initial heating time and k_{SH} is the constant related with thiol surface exposure rate. Kinetic parameters were estimated from experimental results by non-linear regression analysis. Constant k_{SH} was used to study the influence of the three independent variables over thiol surface exposure kinetic during the thermal process.

2.4. Whey protein aggregates design for soy oil emulsion stabilization

Once RSM assays were concluded, three additional WPAg formulations were designed to verify the reliability of the mathematical models adjusted, looking for aggregates with markedly different sizes (350–700 nm), denaturation rates ($t_{1/2}$: 2–14 min), and thiol surface exposure rates (k_{SH}: 4×10^{-2} - 30×10^{-2} min^{-1}) and to evaluate the influence of different protein aggregates on microgel-stabilized emulsions development (Table 4). For each of these test runs, the experimental responses were compared with the responses predicted by the model equations.

The WPAg designed were used to develop stable microgel emulsions based on Destribats et al. (2014). It is worth mentioning that the WPAg designed were obtained as described in section 2.1 without further separation. According to previous studies, WPAg suspensions were diluted at 1% w/w protein content with ultrapure water to ensure that the drop size of the emulsion be independent of the initial stabilizer concentration. The pH of the aqueous dispersions were adjusted at values below, near and above their IEP as suggested by Destribats et al. (2014), using 1 mol L^{-1} HCl or 1 mol L^{-1} NaOH, to evaluate the behavior of the WPAg at the oil-water interface of o/w emulsions as a function of the pH (Table 5). Then, 5 mL of commercial soy oil (AGD, Córdoba, Argentina) together with 5 mL of each WPAg suspension were mixed in a tube and emulsified using a high-speed homogenizer Ultra-Turrax T25 (IKA, Staufen, Germany) operating at 13,500 rpm for 1 min at room temperature (25 °C). The emulsions were prepared in triplicate.

The emulsion stability refers to the ability of an emulsion to resist changes in its properties over time, due to different physicochemical mechanisms including gravitational separation, flocculation, coalescence, Ostwald ripening and phase inversion (McClements, 2007). In the

Table 4
Experimental (mean ± SD, n = 3) and predicted values (Model) for responses Y_1, Y_2, and Y_3 with the error percentage for designed WPAg.

WPAg	Process conditions X_1; X_2; X_3	Y_1 - WPAg size (nm)			Y_2 - $t_{1/2}$ (min)			Y_3 - k_{SH} x10^{-2} (min^{-1})		
		Model	Experimental	Error	Model	Experimental	Error	Model	Experimental	Error
I	71.0 °C; 4.0%; 7.1	352.0	362.6 ± 10.4	3.0%	15.3	13.4 ± 0.8	12.4%	4.54	4.41 ± 0.47	8.9%
II	80.0 °C; 4.3%; 7.5	352.2	364.6 ± 9.8	3.5%	2.1	2.3 ± 0.2	11.9%	29.05	29.82 ± 1.12	2.8%
III	75.7 °C; 5.5%; 6.7	692.8	773.0 ± 8.8	11.6%	5.9	6.4 ± 0.2	8.5%	8.51	7.29 ± 1.78	14.3%

Table 5
Characteristics of soy oil emulsions stabilized by designed WPAg.

Emulsion	WPAg	Protein Conc. (% w/w)	pH	0 day		14 days	
				D[3,2] (μm)	PI	D[3,2] (μm)	PI
E1	I	0.50	3.0	48.2 ± 18.0 [e]	0.763	n.d.*	
E2	I	0.50	4.7	42.2 ± 13.0 [f]	0.464	55.3 ± 16.8 [bc]	0.501
E3	I	0.50	7.0	46.4 ± 11.9 [e]	0.332	54.4 ± 12.8 [cd]	0.285
E4	II	0.50	3.0	61.0 ± 22.5 [a]	0.801	n.d.*	
E5	II	0.50	4.7	42.9 ± 12.4 [f]	0.416	47.0 ± 12.4 [e]	0.374
E6	II	0.50	7.0	56.0 ± 17.0 [bc]	0.472	57.7 ± 18.6 [b]	0.543
E7	III	0.50	3.0	55.2 ± 18.7 [bc]	0.650	n.d.*	
E8	III	0.50	4.7	51.5 ± 16.0 [d]	0.490	54.9 ± 16.2 [bc]	0.357
E9	III	0.50	7.0	55.5 ± 17.1 [bc]	0.450	47.9 ± 15.9 [e]	0.509

D[3,2] values (mean ± SD, n = 200) without a common letter are significantly different (P < 0.05) according to the LSD test.
* D[3,2] and PI values were not determined because significant amounts of emulsion droplets coalesced.

present work, an accelerated stability test was used to analyze the emulsion creaming instability. This procedure may be carried out after by centrifuging an emulsion at a fixed speed for a certain period of time (McClements, 2007). The test was developed based on Dybowska and Krupa-Kozak (2020). Ten mL of each emulsion was centrifuged at 1467 g for 15 min at 25 °C using a Biofuge 28RS centrifuge (Heraeus Sepatech, Osterode, Germany). Then, the volume of the oil released, emulsion phase (cream layer) and the lower aqueous phase (serum layer) were measured.

Also, the droplet size distribution at 0 and 14 days of storage was evaluated to analyze emulsion stability. The size distributions of the drop populations in the emulsion samples were observed with an optical microscope DM750 (Leica Microsystems, Heerbrugg, Switzerland). Digital images were taken and analyzed using ImageJ software (National Institute of Health, Maryland, USA) to measure the diameters of at least 200 droplets to obtain the size distributions of the populations through the surface average diameter (D[3,2]), standard deviation (SD) and the polydispersity index (PI) according to:

$$D[3,2] = \frac{\sum_{i=1}^{N} n_i D_i^3}{\sum_{i=1}^{N} n_i D_i^2} \qquad (7)$$

$$SD = \left[\frac{\left(\sum_{i=1}^{N} \sum n_i D_i^2 \right)\left(\sum_{i=1}^{N} n_i D_i^4 \right)}{\left(\sum_{i=1}^{N} n_i D_i^3 \right)^2} - 1 \right]^{1/2} \qquad (8)$$

$$PI = \frac{1}{D_m} \frac{\sum_{i=1}^{N} n_i D_i^3 |D_m - D_i|}{\sum_{i=1}^{N} n_i D_i^3} \qquad (9)$$

where N is the total number of droplets, n_i is the number of droplets with diameter D_i and D_m is the median diameter.

Finally, confocal laser scanning microscopy (CLSM) was used to study the emulsion droplet morphology. Samples were prepared using 10 μL of Rhodamine B solution (200 μg mL^{-1}) per 1 mL of emulsion to specifically stain WPAg. Then, 30 μL of the labeled samples were placed on a concave microscope glass slide and covered with a glass coverslip. Rhodamine B was excited at 532 nm and detected at 560–600 nm. Images of each emulsion were obtained using an inverted confocal laser scanning microscope Leica TCS SP8 (Leica, Wetzlar, Germany).

3. Results and discussion

3.1. Analysis of thermal aggregation process of whey proteins using response surface methodology

Once that the central-composite design assays were completed, the experimental results were processed to analyze the combined effects of the process variables studied (temperature-X_1, protein concentration-X_2, and pH-X_3), over the three responses evaluated (WPAg size-Y_1, $t_{1/2}$-Y_2, and k_{SH}-Y_3). On each case, a second-order polynomial equation was adjusted, eliminating non-significant terms. The expressions obtained in coded factors for the three responses were:

$$Y_1^{-1.53} = 1.03 \times 10^{-4} - 1.68 \times 10^{-5}X_1 - 1.03 \times 10^{-5}X_2 + 3.62 \times 10^{-5}X_3 + 8.41 \times 10^{-6}X_1X_3 - 1.06 \times 10^{-5}X_3^2 \qquad (10)$$

$$Log(Y_2) = 0.68 - 0.38X_1 + 0.04X_2 + 0.10X_3 - 0.04X_2X_3 + 0.07X_1^2 \qquad (11)$$

$$Log(Y_3) = -0.90 + 0.37X_1 - 8.61 \times 10^{-3}X_2 + 0.16X_3 + 0.06X_2X_3 - 0.19X_1^2 \qquad (12)$$

The responses were transformed to satisfy the ANOVA assumptions (normality and homoscedasticity of residuals). The results of ANOVA show that the RSM developed for the three responses was significant and adequate, without significant lack of fit (Table 2).

A close relationship between the experimental values and the predicted values from model equations shown in Table 3 indicates a good response of the model developed.

Figs. 1–3 show different contour plots obtained with equations (10)–(12), respectively, to analyze the effect of process variables X_1, X_2, and X_3 and their interaction on Y_1, Y_2, and Y_3.

β-lactoglobulin, the main protein in whey, includes 5 cysteine residues on its structure, 4 residues forming disulfide bonds and one is a free
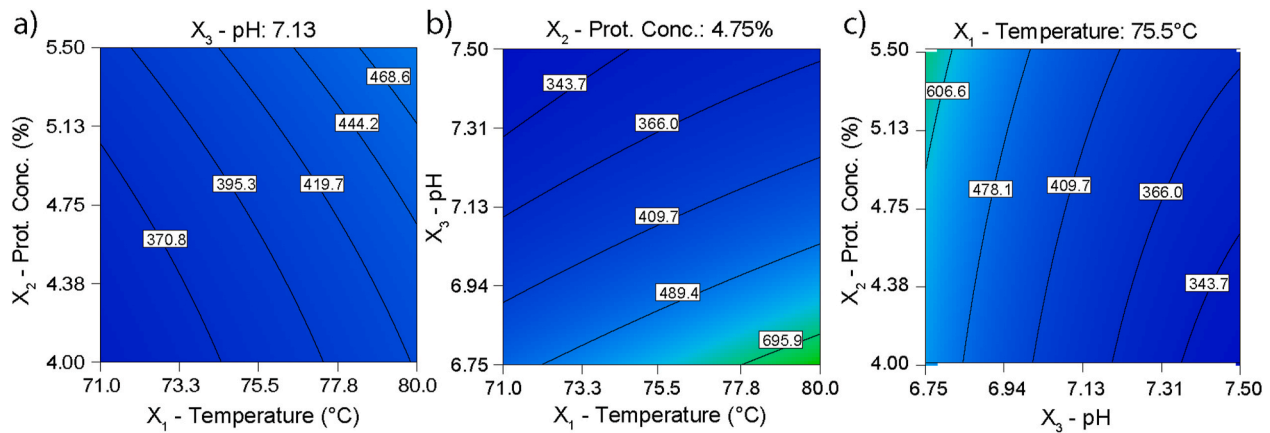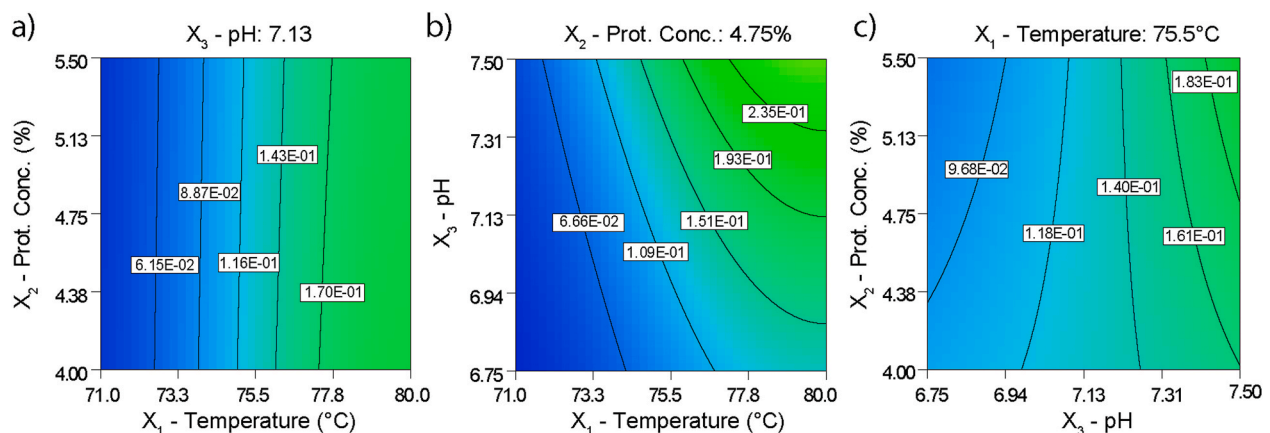
Fig. 1. Contour plot showing the combined effect of: (a) X_2 - protein concentration (% w/w) and X_1 - temperature (°C); (b) X_3 - pH and X_1 - temperature (°C); (c) X_2 - protein concentration (% w/w) and X_3 - pH, on Y_1 - WPAg size (nm).
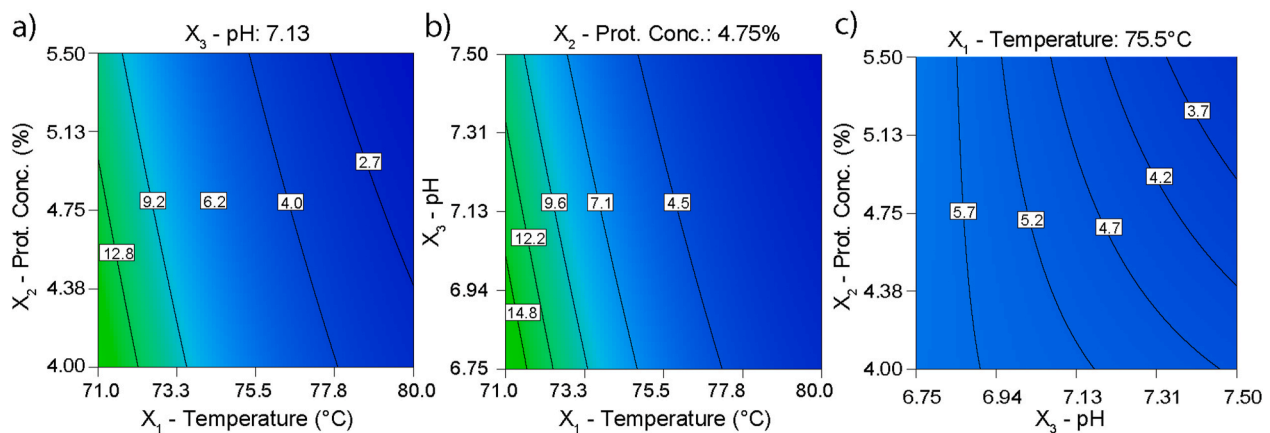
Fig. 2. Contour plot showing the combined effect of: (a) X_2 - protein concentration (% w/w) and X_1 - temperature (°C); (b) X_3 - pH and X_1 - temperature (°C); (c) X_2 - protein concentration (% w/w) and X_3 - pH, on Y_2 - $t_{1/2}$ (min).

Fig. 3. Contour plot showing the combined effect of: (a) X_2 - protein concentration (% w/w) and X_1 - temperature (°C); (b) X_3 - pH and X_1 - temperature (°C); (c) X_2 - protein concentration (% w/w) and X_3 - pH, on Y_3 - k_{SH} (min^{-1}).

thiol group. Throughout thermal treatment, the reactivity of the free thiol group can be markedly increased by protein unfolding, promoting SH/S-S interchange reactions with cysteine residues of the same or of another protein molecule. This mechanism plays an important role in the heat-induced aggregation and gelation of whey protein suspensions (Sava et al., 2005). Thus, among the process conditions analyzed, it can be observed that higher temperature conditions promote the thiol

surface exposure rate, WP denaturation rate, and WPAg size increment (Fig. 1a and b; Fig. 2a and b; Fig. 3a and b).

As pH value gets closer to WP IEP, protein surface charges are screened, reducing repulsion and promoting non-covalent interactions (Stănciuc, Dumitraşcu, Ardelean, Stanciu, & Râpeanu, 2012). Instead, at pH values above WP IEP, intramolecular charge repulsion increases, thus intermolecular aggregation is less favored. However, since the pKa

of the cysteine sulfhydryl is about 8, increasing pH promotes thiol reactivity and the denaturation/aggregation reaction rates (Ryan et al., 2013). According to the results obtained, pH increments lead to smaller WPAg and higher WP denaturation and surface thiol exposure rates (Fig. 1b and c; Fig. 2b and c; Fig. 3b and c).

It was previously established that protein aggregation begins at concentrations above a critical association concentration, where primary aggregates are formed and may further aggregate into larger arrangements (Mehalebi, Nicolai, & Durand, 2008). Thus, as WP concentration increases, in the range evaluated, large aggregates production is more likely because the collision probability between molecules is increased (protein-protein or aggregate-aggregate) (Fig. 1a and c). Instead, in the temperature range evaluated, protein unfolding rate and intermolecular disulfide formation seem to be fast enough not to show a dependence on protein concentration (Iametti, Cairoli, De Gregori, & Bonomi, 1995), so WP concentration showed a limited effect on the thiol surface exposure rate (Fig. 3a and c) and on the WP denaturation rate (Fig. 2a and c).

The results evidence that WP aggregation under thermal treatments is a complex process driven by the interaction between different variables. Thus, it is not only important to evaluate the influence of each variable over the aggregation process separately, but also their combined overall effect at different levels. Therefore, the development of mathematical models integrating the effects of the most relevant process variables over WP aggregation is a key instrument to obtain suitable WPAg for stable emulsion design.

3.2. Emulsion preparation and characterization using whey protein aggregates designed by RSM

To validate the reliability of the mathematical models adjusted with RSM, three additional formulations were generated to obtain WPAg with markedly different characteristics (section 2.4). For each of these test runs, the experimental responses were compared with the responses predicted by the mathematical models. Table 4 shows the process conditions of the proposed formulations and the experimental and predicted values for the three response variables (in triplicate) along with the calculated error percentage.

All three responses evaluated (Y_1, Y_2, and Y_3) of the three additional WPAg formulations showed a good correlation between experimental and predicted values, indicating the robustness of the mathematical models adjusted.

Whey protein aggregates developed by the RSM models (Table 4) were used to obtain nine different soy oil emulsions as described in Table 5. After the thermal treatment and before the emulsification process, the fractions of soluble/insoluble protein remained in WPAg suspensions were evaluated according to section 2.3.2. The insoluble protein fraction presents in WPAg suspensions I, II and III were 90.3 ± 1.0%, 100.4 ± 0.6% and 89.9 ± 1.3% respectively.

The structure of the microgel adsorbed layer at the oil/water interface influences the long-term emulsion structural integrity. Thus, the effects of pH, WPag characteristics, and storage time on emulsion stability were studied. During the accelerated stability test, emulsions separated into two (no release of oil on the top of the samples) or three (significant amounts of oiling off) visible phases. Fig. 4 shows the oil/emulsion/aqueous phase volume percentage distribution of the soy oil emulsions designed, at the initial day (Fig. 4a) and after two weeks (Fig. 4b) of storage at room temperature.

The study showed that emulsions generated at pH 3 (E1, E4 and E7) presented significant amounts of oil released after the centrifugation protocol (Fig. 4). Besides, the size distribution of the drop populations in these emulsions presented the highest initial values of PI (Table 5), i.e., an early sign of emulsion instability possible associated with lower/incomplete adsorption of the WPAg on the interface of droplets (Kuhn & Cunha, 2012). After the 14 days of storage these emulsions showed clear signs of coalescence, making impossible the determination of D[3,2] and
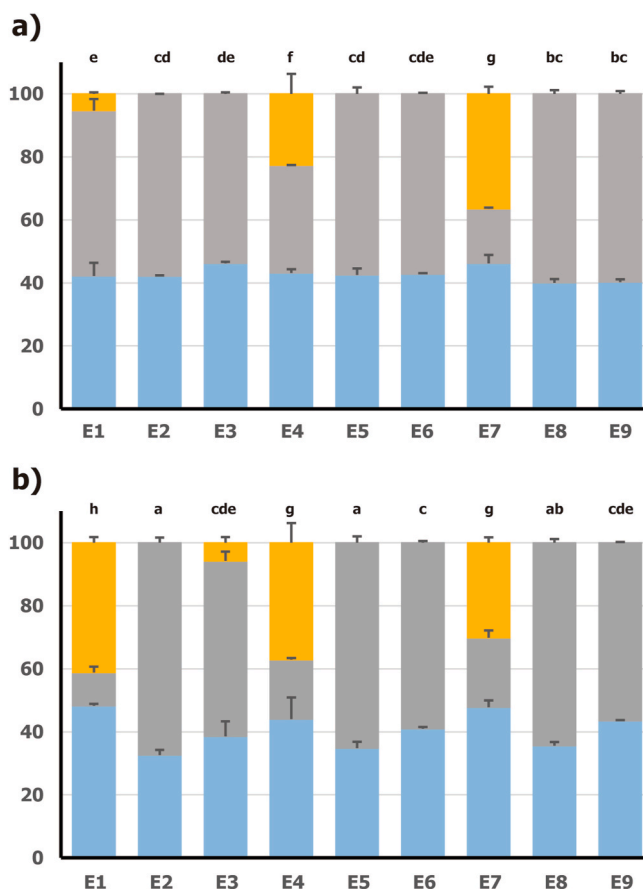

Fig. 4. Volume percentage distribution of oil (orange), emulsion (grey) and aqueous phase (light blue) of soy oil emulsions at 0 (a) and 14 days (b) of storage at room temperature. Error bars denote standard deviation of three independent measurements. Emulsion columns without a common letter are significantly different (P < 0.05) according to the LSD test. (For interpretation of the references to colour in this figure legend, the reader is referred to the Web version of this article.)

PI values. Instead, emulsions generated at pH 7 (E3, E6 and E9), maintained the initial emulsion phase volume constant (P < 0.05) after the storage period with either of the different protein aggregates (Fig. 4). This opposite behavior can be explained taking into account that WPAg present a polyampholyte character, making colloidal stability of the soy oil emulsions be highly influenced by their overall charge. An asymmetric swelling behavior was reported on either side of the IEP (Destribats et al., 2014), being more pronounced at acidic pH because of the distribution and degree of ionization of the lateral carboxyl and amino groups of the protein amino acids, which could contribute to emulsions instability. However, since the pKa of the cysteine sulfhydryl is about 8, disulfide bond formation is enhanced at high pH promoting thiol reactivity (Ryan et al., 2013). Thus, the cross-linking between the proteins in the continuous phase and adsorbed proteins on the oil droplets during emulsification could enhance emulsion stability when pH is above IEP (Dickinson, 2012).

Microgel-stabilized emulsions developed at pH 4.7 (E2, E5 and E8) showed no oil release after the centrifugation process and presented the same emulsion phase volume (P < 0.05) using any of the three different protein aggregates at the beginning of the storage period (Fig. 4a). After 14 days, the emulsion phase volume of E2, E5 and E8 increases (P < 0.05), but remains equal for either of them (Fig. 4b). Moreover, these emulsions presented a smaller drop diameter (P < 0.05) than those obtained at pH 3 and 7 at the onset of the storage period (Table 5). However, the D[3,2] value of E2, E5 and E8 slightly increased at 14 days of storage P < 0.05). In Fig. 5, CLSM images from soy oil emulsions
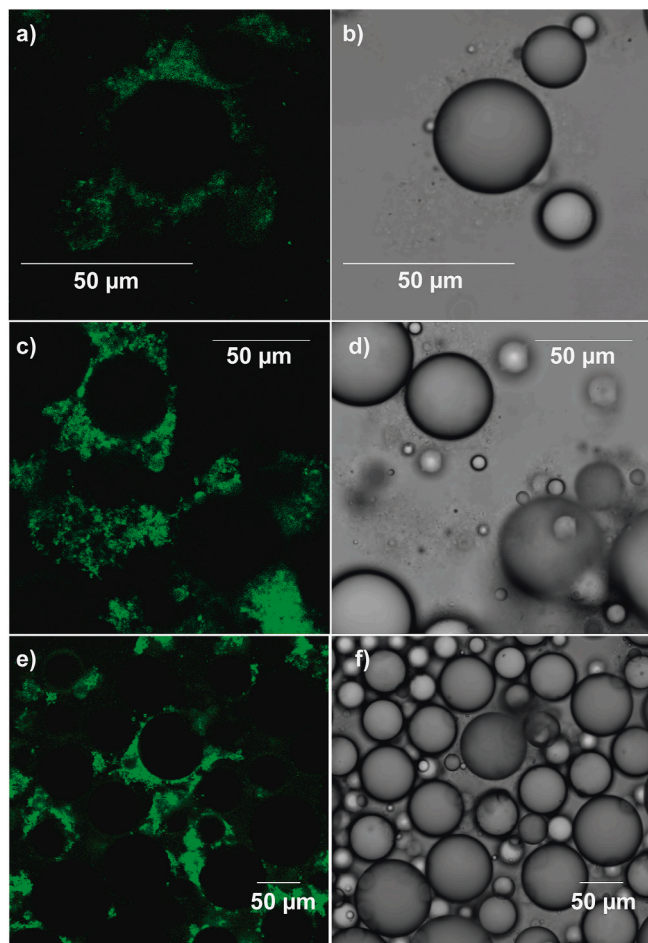
Fig. 5. Confocal laser scanning microscopy images of emulsions E2 (a, b), E5 (c, d) and E8 (e, f). Rhodamine B staining shows WPAg network adsorption at the oil drops (a, c and e).

stabilized by WPAg at pH 4.7 are shown. The WPAg distribution surrounding the oil droplets forming a thick layer and bridging the neighboring drops can be visualized by the fluorescent dye Rhodamine B (Fig. 5a, c and e).

The microgel particles exhibit self-aggregation near the IEP (pH ∼ 4.8), forming a structured network of aggregated particles in the aqueous continuous phase leading to flocculation of droplets by protein bridging without droplet coalescence (Dickinson, 2017). Thus, a clear aqueous phase is observed because most of the WPAg are adsorbed on the oil drop surface forming a dense network (Destribats et al., 2014). However, when emulsion pH is far from the IEP (pH 3 and 7), the subnatant is turbid suggesting that an important fraction of the WPAg remained non-adsorbed in the aqueous phase (Dybowska & Krupa-Kozak, 2020).

4. Conclusions

In the present work, we have investigated the thermal aggregation process of WPC suspensions, analyzing the effects of temperature, protein concentration, and pH conditions on the characteristics of the protein aggregates developed. Different mathematical models were adjusted through RSM to correlate the influence of process variables on WPAg size, protein denaturation rate, and thiol surface exposure rate during the thermal aggregation process. The models were used to design three different WPAg formulations to generate stable food-grade microgel emulsions at three pH conditions. Significant relationships between pH, WPAg characteristics, and storage time on the stability of

soy oil emulsions, were found. Emulsions generated at pH 4.7 and 7 using the three different WPAg, exhibited high resistance to coalescence as demonstrated by the accelerated stability test assayed. On the other hand, emulsions generated at pH 3 were unstable, presenting high amounts of oil released after 14 days of storage with either of the WPAg designed.

Further investigation about the development of microgel-stabilized emulsions using different types of WPAg will be useful to gain a better general understanding of whey protein aggregates applications for encapsulation of lipophilic bioactive materials towards healthy functional food design.

CRediT authorship contribution statement

Ignacio Niizawa: Writing – original draft, Conceptualization, Methodology, Validation, Software, Formal analysis, Visualization. **Guillermo A. Sihufe:** Resources, Supervision, Writing – review & editing, Project administration, Funding acquisition. **Susana E. Zorrilla:** Conceptualization, Methodology, Supervision, Writing – review & editing, Resources, Project administration, Funding acquisition.

Declaration of competing interest

The authors declare that they have no known competing financial interests or personal relationships that could have appeared to influence the work reported in this paper.

Acknowledgments

References

Büchi Labortechnik, A. G. (1998). *Nitrogen determination according to Kjeldahl, order No. 97765*. Switzerland: Büchi, Flawil.

Destribats, M., Rouvet, M., Gehin-Delval, C., Schmitt, C., & Binks, B. P. (2014). Emulsions stabilised by whey protein microgel particles: Towards food-grade pickering emulsions. *Soft Matter, 10*(36), 6941–6954. https://doi.org/10.1039/C4SM00179F

Dickinson, E. (2012). Emulsion gels: The structuring of soft solids with protein-stabilized oil droplets. *Food Hydrocolloids, 28*(1), 224–241. https://doi.org/10.1016/j.foodhyd.2011.12.017

Dickinson, E. (2015). Microgels – an alternative colloidal ingredient for stabilization of food emulsions. *Trends in Food Science & Technology, 43*, 178–188. https://doi.org/10.1016/j.tifs.2015.02.006

Dickinson, E. (2017). Biopolymer-based particles as stabilizing agents for emulsions and foams. *Food Hydrocolloids, 68*, 219–231. https://doi.org/10.1016/j.foodhyd.2016.06.024

Dybowska, B. E., & Krupa-Kozak, U. (2020). Stability of oil-in-water emulsions as influenced by thermal treatment of whey protein dispersions or emulsions. *International Journal of Dairy Technology, 73*(3), 513–520. https://doi.org/10.1111/1471-0307.12689

Iametti, S., Cairoli, S., De Gregori, B., & Bonomi, F. (1995). Modifications of high-order structures upon heating of β-lactoglobulin: Dependence on the protein concentration. *Journal of Agricultural and Food Chemistry, 43*, 53–58. https://doi.org/10.1021/jf00049a011

Kuhn, K. R., & Cunha, R. L. (2012). Flaxseed oil – whey protein isolate emulsions: Effect of high pressure homogenization. *Journal of Food Engineering, 111*(2), 449–457. https://doi.org/10.1016/j.jfoodeng.2012.01.016

Li-Chan, E. (1983). Heat-induced changes in the proteins of whey protein concentrate. *Journal of Food Science, 48*, 47–56. https://doi.org/10.1111/j.1365-2621.1983.tb14786.x

McClements, D. J. (2007). Critical review of techniques and methodologies for characterization of emulsion stability. *Critical Reviews in Food Science and Nutrition, 47*(7), 611–649. https://doi.org/10.1080/10408390701289292

Mehalebi, S., Nicolai, T., & Durand, D. (2008). Light scattering study of heat-denatured globular protein aggregates. *International Journal of Biological Macromolecules, 43*, 129–135. https://doi.org/10.1016/j.ijbiomac.2008.04.002

Meza, B. E., De Piante Vicín, D. A., Marino, F., Sihufe, G. A., Peralta, J. M., & Zorrilla, S. E. (2020). Characterisation of soluble aggregates from commercial whey

protein concentrate suspensions: Effect of protein concentration, pH, and heat treatment conditions. *International Journal of Dairy Technology, 73*(2), 429–436. https://doi.org/10.1111/1471-0307.12669

Meza, B. E., Verdini, R. A., & Rubiolo, A. C. (2009). Viscoelastic behavior of heat-treated whey protein concentrates suspensions. *Food Hydrocolloids, 23*, 661–666. https://doi.org/10.1016/j.foodhyd.2008.03.015

Mourouzidis-Mourouzis, S. A., & Karabelas, A. J. (2006). Whey protein fouling of microfiltration ceramic membranes—pressure effects. *Journal of Membrane Science, 282*, 124–132. https://doi.org/10.1016/j.memsci.2006.05.012

Murphy, R. W., Zhu, L., Narsimhan, G., & Jones, O. G. (2018). Impacts of size and deformability of β-Lactoglobulin microgels on the colloidal stability and volatile flavor release of microgel-stabilized emulsions. *Gels, 4*(3), 79. https://doi.org/10.3390/gels4030079

Nicolai, T. (2016). Formation and functionality of self-assembled whey protein microgels. *Colloids and Surfaces B: Biointerfaces, 137*(1), 32–38. https://doi.org/10.1016/j.colsurfb.2015.05.055

Nicolai, T., Britten, M., & Schmitt, C. (2011). β-Lactoglobulin and WPI aggregates: Formation, structure and applications. *Food Hydrocolloids, 25*(8), 1945–1962. https://doi.org/10.1016/j.foodhyd.2011.02.006

Nicolai, T., & Durand, D. (2013). Controlled food protein aggregation for new functionality. *Current Opinion in Colloid & Interface Science, 18*(4), 249–256. https://doi.org/10.1016/j.cocis.2013.03.001

Ramos, O. L., Pereira, R. N., Martins, A., Rodrigues, R., Fuciños, C., Teixeira, J. A., et al. (2017). Design of whey protein nanostructures for incorporation and release of nutraceutical compounds in food. *Critical Reviews in Food Science and Nutrition, 57*(7), 1377–1393. https://doi.org/10.1080/10408398.2014.993749

Ryan, K. N., & Foegeding, E. A. (2015). Formation of soluble whey protein aggregates and their stability beverages. *Food Hydrocolloids, 43*, 265–274. https://doi.org/10.1016/j.foodhyd.2014.05.025

Ryan, K. N., Zhong, Q., & Foegeding, E. A. (2013). Use of whey protein soluble aggregates for thermal stability-a hypothesis paper. *Journal of Food Science, 78*(8), 1105–1115. https://doi.org/10.1111/1750-3841.12207

Sarkar, A., Murray, B., Holmes, M., Ettelaie, R., Abdalla, A., & Yanga, X. (2016). In vitro digestion of pickering emulsions stabilized by soft whey protein microgel particles: Influence of thermal treatment. *Soft Matter, 12*, 3558–3569. https://doi.org/10.1039/C5SM02998H

Sava, N., Van der Plancken, I., Claeys, W., & Hendrickx, M. (2005). The kinetics of heat-induced structural changes of β-lactoglobulin. *Journal of Dairy Science, 88*, 1646–1653. https://doi.org/10.3168/jds.S0022-0302(05)72836-8

Schmitt, C., Bovay, C., Vuilliomenet, A. M., Rouvet, M., & Bovetto, L. (2011). Influence of protein and mineral composition on the formation of whey protein heat-induced microgels. *Food Hydrocolloids, 25*, 558–567. https://doi:10.1016/j.foodhyd.2010.05.010.

Stănciuc, N., Dumitraşcu, L., Ardelean, A., Stanciu, S., & Râpeanu, G. (2012). A kinetic study on the heat-induced changes of whey proteins concentrate at two pH values. *Food and Bioprocess Technology, 5*, 2160–2171. https://doi.org/10.1007/s11947-011-0590-y

Wijayanti, H. B., Bansal, N., & Deeth, H. C. (2014). Stability of whey proteins during thermal processing: A review. *Comprehensive Reviews in Food Science and Food Safety, 14*, 1235–1251. https://doi.org/10.1111/1541-4337.12105

de Wit, J. N. (1990). Thermal stability and functionality of whey proteins. *Journal of Dairy Science, 73*(12), 3602–3612. https://doi.org/10.3168/jds.S0022-0302(90)79063-7

Zhang, Z., Arrighi, V., Campbell, L., Lonchamp, J., & Euston, S. R. (2016). Properties of partially denatured whey protein products: Formation and characterisation of structure. *Food Hydrocolloids, 52*, 95–105. https://doi.org/10.1016/j.foodhyd.2015.06.009

Zou, L., & Akoh, C. C. (2013). Characterisation and optimisation of physical and oxidative stability of structured lipid-based infant formula emulsion: Effects of emulsifiers and biopolymer thickeners. *Food Chemistry, 141*(3), 2486–2494. https://doi.org/10.1016/j.foodchem.2013.05.029